American Mineralogist, Volume 87, pages 739–744, 2002

Ciprianiite and mottanaite-(Ce), two new minerals of the hellandite group from Latium (Italy)

GIANCARLO DELLA VENTURA,[1] PAOLA BONAZZI,[2] ROBERTA OBERTI,[3,*] AND LUISA OTTOLINI[3]

[1] Dipartimento di Scienze della Terra, Università della Calabria, I-87030 Arcavacata di Rende (CS), Italy
[2] Dipartimento di Scienze della Terra, Università di Firenze, I-50121 Firenze, Italy
[3] CNR-CS per la Cristallochimica e la Cristallografia (CSCC), via Ferrata 1, I-27100 Pavia, Italy

ABSTRACT

Two new minerals of the hellandite group were found within alkali-syenitic ejecta enclosed in pyroclastic formations of the Roman Comagmatic Province (Latium, Italy). Mottanaite-(Ce) [ideally $^{X}Ca_4^{Y}(CeCa)^{Z}Al^{T}Be_2(Si_4B_4O_{22})^{W}O_2$] and ciprianiite [ideally $^{X}Ca_4^{Y}[(Th,U)(REE)]^{Z}Al^{T}\square_2(Si_4B_4O_{22})^{W}(OH, F)_2$] occur as transparent, brown-colored, tabular euhedral crystals in miarolitic cavities and voids of the ejecta, which consist mainly of sanidine and plagioclase (An ranging from 20 to 80%), with minor amounts of feldspathoid, clinopyroxene and/or clinoamphibole, magnetite, titanite, and zircon. Locally, accessory minerals include britholite-(Ce), baddeleyite, phosphate to silico-phosphate phases close in composition to the brabantite-cheralite series, thorite, fluorite, danburite, and vonsenite. The genesis of the new hellandite end-members can be related to late-stage post magmatic hydrothermal fluids enriched in Zr, Ti, REEs, and actinide elements.

Both mottanaite-(Ce) and ciprianiite have a vitreous luster and are non-fluorescent. Cleavage is absent in mottanaite-(Ce), fair to good in ciprianiite, {100}. Twinning is frequently observed in ciprianiite. Due to the strong intra-crystalline chemical zoning and twinning, physical properties could be measured only for mottanaite-(Ce). D_{meas} is 3.61(4) g/cm^3, D_{calc} is 3.88 g/cm^3. Mottanaite-(Ce) is biaxial negative, with α = 1.680(5), β = 1.694(2), γ = 1.708(5); $2V_{meas}$ ~90°.

Both minerals are monoclinic, space group *P*2/*a*, *Z* = 2. Unit-cell parameters for the crystals studied are: *a* = 19.032(9) Å, *b* = 4.746(3) Å, *c* = 10.248(5) Å, β = 110.97(5)°, *V* = 864.3(8) Å^3 for mottanaite-(Ce), and *a* = 19.059(5) Å, *b* = 4.729(1) Å, *c* = 10.291(4) Å, β = 111.33(2)°, *V* = 864.0(5) Å^3 for ciprianiite. Single-crystal structure refinement confirmed the presence of a further distorted tetrahedral site which was first detected in a hellandite-(Ce) sample from Latium (Oberti et al. 1999). This site is occupied by Be (±Li) in stoichiometric mottanaite-(REE), whereas it mainly hosts hydrogen (bonded to the O5 oxygen atom) in ciprianiite and hellandite-(REE); solid solution between the end-members is possible, as shown by the studied samples. The chemical composition of the refined crystals was obtained by combining EMPA (for medium-*Z* elements) and SIMS analyses (for low- and high-*Z* elements); their results are in excellent agreement with the chemical information obtained from the structure refinements. The crystal-chemical formulae of the crystals studied, recalculated on the basis of 24 anions, are $^{M3,4}Ca_4^{M2}[REE_{1.45}Ca_{0.37}(Th,U)^{4+}_{0.17}Y_{0.01}]_{\Sigma=2}{}^{M1}(Al_{0.50}Fe^{3+}_{0.38}Mg_{0.03}Ti^{4+}_{0.07})_{\Sigma=0.99}{}^{T}(Be_{1.18}Li_{0.02}\square_{0.37})B_{3.99}Si_{3.98}O_{22}{}^{O5}(O^{2-}_{1.04}F_{0.53}OH_{0.43})_{\Sigma=2}$ for mottanaite-(Ce); and $^{M3,4}Ca_4{}^{M2}[REE^{3+}_{0.72}(Th,U)^{4+}_{0.66}Ca_{0.60}Y_{0.02}]_{\Sigma=2}{}^{M1}(Al_{0.48}Fe^{3+}_{0.38}Ti^{4+}_{0.10}Mg_{0.05}Mn^{3+}_{0.02})_{\Sigma=1.03}{}^{T}(Be_{0.82}\square_{0.60}Li_{0.04})B_{4.00}Si_{4.00}O_{22}{}^{O5}(O^{2-}_{0.97}OH_{0.54}F_{0.49})_{\Sigma=2}$ for ciprianiite.

INTRODUCTION

Hellandite is a rare borosilicate mineral, first found at Kragerö (Norway) by Brögger (1903) and studied by Brögger (1907, 1922) and by Oftedal (1964, 1965). The structure was later determined by Mellini and Merlino (1977) using a sample from Predazzo (Italy). A few other occurrences were reported over the past two decades, including the very recent description of hellandite-(Ce) (Oberti et al. 1999 and references therein). The discovery of several non-metamict hellandite samples from the volcanic Plio-Pleistocene potassic province of Latium (the so-called Roman Comagmatic Region; Washington 1906) prompted a detailed study of the crystal chemistry of the hellandite-group minerals using a combination of microchemical (SEM-EDX, EMPA, SIMS), single-crystal X-ray diffraction, and spectroscopic (IR) methods. The collected data, together with a critical re-evaluation of the existing data on hellandites, permits the clarification of several previously unresolved problems, such as the relations between hellandite and tadzhikite, the presence of vacancies and OH groups in the structure, and a general crystal-chemical formula for these minerals. The redefinition of the hellandite group that resulted from these studies has been approved by the International Mineralogical Association (IMA) commission and is published in a companion paper (Oberti et al. 2002).

In this paper we report the occurrence of two new end-members of the hellandite group found in syenitic ejecta scattered throughout the pyroclastic formations of the Latium volcanic province. The new minerals and mineral names have been approved by the Commission on New Minerals and Mineral

* E-mail: oberti@crystal.unipv.it

Names (CNMMN) of the IMA.

The name ciprianiite is after Curzio Cipriani, Professor of Mineralogy and Head of the Museum of Mineralogy, later of Natural History, at the Università di Firenze (Italy), in recognition of his contribution to mineral systematics. Holotype material for ciprianiite has been deposited at the Museo di Storia Naturale, Università di Firenze (Department of Mineralogy) under the catalogue number 2771/RI.

The name mottanaite is after Annibale Mottana, Professor of Mineralogy at the University of Roma Tre (Italy), in recognition of his leadership and support of investigations and cataloguing of the Latium minerals, during which the mottanaite-(Ce) sample was found (a Levinson modifier is added according to the new guidelines for the hellandite group). Holotype material for mottanaite-(Ce) has been deposited at Museo di Mineralogia, Università di Roma "La Sapienza" under the catalogue number 30023/1.

Occurrence and physical properties

Mottanaite-(Ce) occurs within a feldspathoid-bearing alkali-syenitic ejectum sampled from the "lower pyroclastic flow" of the Sabatini volcanic complex (De Rita et al. 1983), outcropping at Monte Cavalluccio, Sacrofano, north of Rome. The host rock ("type-A" ejectum, Della Ventura et al. 1992) is composed of predominant sanidine and plagioclase (An ranging from 20 to 80%) with minor nepheline. Microscopically the rock shows a hornfels-like texture consisting of a skeleton of large platy K-feldspar crystals with clinopyroxene (aegirine-augite), titanian andradite, magnetite, biotite, and nepheline as minor phases. Several accessory phases including zircon, titanite, baddeleyite (Fig. 1a), and silico-phosphates of Th, U, and REEs close in composition to cheralite-brabantite (Fig. 1b) were identified by SEM-EDX (Philips XL30 microscope, equipped with a solid-state super-UTW EDX detector, at LIME: Laboratorio Interdipartimentale di Microscopia Elettronica, University of Roma Tre). Mottanaite-(Ce) occurs in miarolitic cavities and voids (Fig. 1c) where it is frequently intergrown with britholite-(Ce) (Fig. 1d), as in the case of hellandite-(Ce) from Capranica (Della Ventura et al. 1999b).

Ciprianiite occurs within a syenitic ejectum collected at Tre Croci, close to Vetralla (Viterbo province) within a pyroclastic formation belonging to the Vico volcanic complex (Bernabè 1987). The host rock is composed of sanidine, plagioclase (An ranging from 20 to 80%), hornblende, and magnetite. Accessory phases include titanite and zircon. Ciprianiite occurs in miarolitic cavities associated with danburite, thorite, fluorite, tourmaline, and a cancrinite-group mineral.

Both mottanaite-(Ce) and ciprianiite occur as small (<0.5 mm) tabular ({010} dominant) crystals, brown to pale brown in color, translucent to transparent, with vitreous luster. Streak is white. Fluorescence was not observed. Both minerals are brittle, with conchoidal fracture. Cleavage {100} is fair to good in ciprianiite, but absent in mottanaite-(Ce). Ciprianiite is frequently twinned on {100}.

In both minerals, as well as in the other studied hellandite-group samples from Latium (Oberti et al. 2002), large inter- and intra-crystalline chemical variations are observed. These variations are always crystal-chemically related, and should thus be ascribed to the composition of the fluid from which the crystals grew. For this reason, and considering that hellandite occurs as rare crystals typically intergrown with britholite or other REE bearing phases (e.g., Della Ventura et al. 1999b), the determination of the optical and physical properties is often very difficult or impossible. In the case of ciprianiite, twinning makes optical measurements more difficult. These data could be determined only for mottanaite-(Ce); due to the similarity in structure and composition, they can also be used, with a reasonable degree of confidence, for ciprianiite and hellandite-(Ce).

Density and the optical properties for mottanaite-(Ce) were determined on a second grain, hand-picked from the same rock

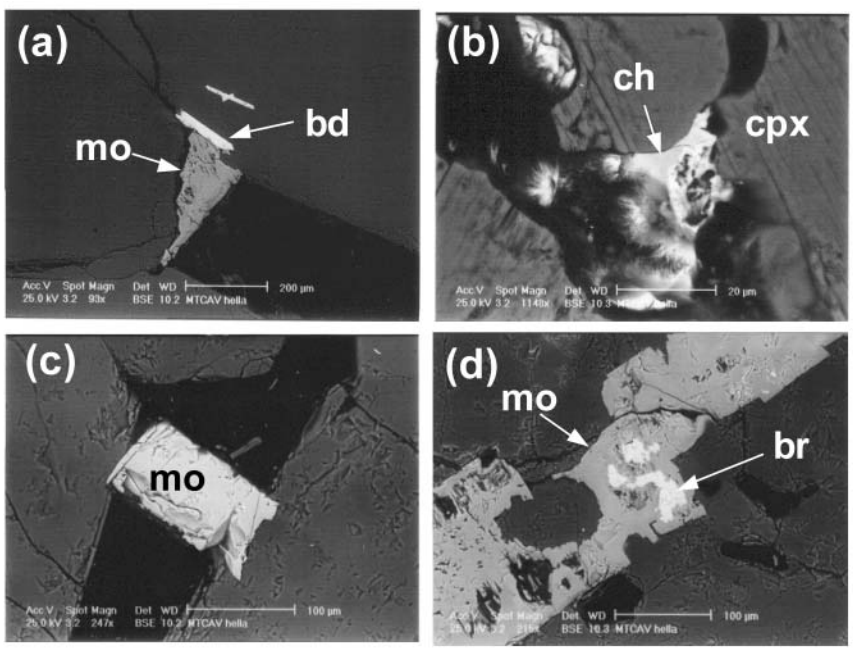

Figure 1. SEM-BSE images of (**a**) a mottanaite-(Ce) crystal (mo) between intersecting K-feldspar crystals, associated with acicular baddeleyite (bd); (**b**) a silico-phosphate of U, Th, and REE (ch) between early formed clinopyroxene and K-feldspar crystals; (**c**) a euhedral mottanaite-(Ce) crystal in a cavity between intersecting K-feldspar crystals; (**d**) mottanaite-(Ce) intergrown with britholite (br).

specimen as the crystal used for structure refinement and microchemical analysis. D_{meas}, determined at room temperature by suspension in Clerici solution, is 3.61(4) g/cm^3, and can be compared with D_{calc} = 3.88 g/cm^3. Optically, mottanaite-(Ce) is non-pleochroic, biaxial negative, with α = 1.680(5), β = 1.694(2), γ = 1.708(5); $2V \sim 90°$. When using the density value measured on the same crystal used for the optical measurements (D = 3.61), $1 - (K_P/K_C) = -0.021$, and the compatibility (Gladstone-Dale, calculated according to Mandarino 1981) is excellent. When using the density value calculated from the structure refinement (thus on a different crystal from the same rock sample, D = 3.88), $1 - (K_P/K_C) = -0.089$, and the compatibility is poor. This behavior is consistent with the strong compositional variation discussed above.

X-RAY CRYSTALLOGRAPHY AND IR SPECTROSCOPY

Diffraction data for mottanaite-(Ce) were collected on a Philips PW-1100 four-circle diffractometer working with graphite-monochromatized Mo$K\alpha$ X-radiation. Unit-cell dimensions were calculated from least-squares refinement of the d values obtained from 50 rows of the reciprocal lattice by measuring the centroid of gravity of each reflection and of the corresponding antireflection in the range $-30 < \theta < 30°$. Intensity data were collected for the monoclinic-equivalent pairs (hkl and $h\bar{k}l$) in the range $2 < \theta < 30°$, and corrected for absorption, Lorentz, and polarization effects; equivalent reflections were then merged and structure factors were calculated. Structure-refinement procedures on the reflections with $I \geq 3\ \sigma(I)$ were as described in Oberti et al. (1999).

For ciprianiite, diffraction data were collected on an Enraf Nonius CAD4 single-crystal diffractometer working with graphite-monochromatized Mo$K\alpha$ X-radiation. Unit-cell dimensions were calculated by least-squares refinement using 25 reflections ($17 < \theta < 26°$). Intensity data were collected for the monoclinic-equivalent pairs (hkl and $\bar{h}\bar{k}l$) in the range $2 < \theta < 35°$. Intensities were then corrected for absorption, Lorentz, and polarization effects; equivalent reflections were averaged and reduced to structure factors. Structure refinement was performed using the program SHELXL93 (Sheldrick 1993). As with mottanaite-(Ce), scattering curves for fully ionized chemical species were used at sites where chemical substitutions occur.

Selected crystal data are provided in Table 1, atomic coordinates, equivalent isotropic atom displacement parameters (adp), and refined site-scattering (ss) values are provided in Table 2, selected geometric parameters in Table 3. Tables 4 and 5, containing the observed and calculated structure factors and the anisotropic components of the adps, respectively, have been deposited[1]. The calculated X-ray powder patterns are provided in Table 6.

TABLE 1. Unit-cell dimensions and crystal-structure information

	mottanaite-(Ce)	ciprianiite
a (Å)	19.032(9)	19.059(5)
b (Å)	4.746(3)	4.729(1)
c (Å)	10.248(5)	10.291(4)
β (°)	110.97(5)	111.33(2)
V (Å^3)	864.3(8)	864.0(5)
Space group	$P2/a$	$P2/a$
θ range (°)	2–30	2–35
no. all	2819	3806
no. obs	1994	2809
R_{sym} (%)	1.6	3.1
R_{all} (%)	7.6	5.5
R_{obs} (%)	6.2	3.2

[1] For a copy of Tables 4 and 5, document item AM-02-010, contact the Business Office of the Mineralogical Society of America (see inside front cover of recent issue) for price information. Deposit items may also be available on the American Mineralogist web site at http://www.minsocam.org.

TABLE 2. Atom fractional coordinates, equivalent isotropic displacement parameters (Å^2) and refined site-scattering (ss; epfu) for mottanaite-(Ce) and ciprianiite

	mottanaite-(Ce)					ciprianiite				
	ss	x/a	y/a	z/c	B_{eq}	ss	x/a	y/a	z/c	B_{eq}
B1	10.0	0.1732(7)	0.5316(25)	0.4513(11)	0.56(26)	10.0	0.1733(2)	0.5268(8)	0.4515(4)	0.75(5)
B2	10.0	0.2542(6)	0.4670(26)	0.1331(11)	0.44(25)	10.0	0.2529(2)	0.4618(8)	0.1329(4)	0.71(5)
Si1	28.0	0.1039(1)	0.4834(8)	0.6508(3)	0.50(6)	28.0	0.1039(1)	0.4849(2)	0.6501(1)	0.64(2)
Si2	28.0	0.1126(2)	0.4992(8)	0.1612(3)	0.55(6)	28.0	0.1127(1)	0.4975(2)	0.1616(1)	0.71(2)
T	2..2	0.0393(5)	0.5424(20)	0.8668(10)	0.92(42)	2.5	0.038(1)	0.535(4)	0.869(2)	1.41(20)
M1	18.4	0	0	0	0.74(7)	18.2	0	0	0	0.73(2)
M2	110.0	0.0424(1)	0.0149(1)	0.3612(1)	0.56(2)	115.7	0.0429(1)	0.0175(1)	0.3598(1)	0.66(1)
M3	41.7	0.2471(1)	0.0032(5)	0.6614(2)	0.72(5)	41.9	0.2476(1)	0.0017(1)	0.6611(1)	0.88(2)
M4	43.3	0.1570(1)	-0.0285(5)	0.9314(2)	0.85(5)	53.7	0.1564(1)	0.9652(1)	0.9312(1)	0.85(1)
H						0.5	0.04(1)	0.42(4)	0.90(2)	1.6
O1		0.0443(4)	0.2410(19)	0.5674(8)	0.73(20)		0.0444(1)	0.2441(5)	0.5673(3)	0.85(4)
O2		0.1778(4)	0.3191(18)	0.7546(8)	0.70(20)		0.1786(1)	0.3179(5)	0.7584(3)	0.87(4)
O3		0.0697(5)	–0.3100(20)	0.7410(10)	1.52(25)		0.0715(1)	0.6991(6)	0.7351(3)	1.32(4)
O4		0.1320(5)	–0.3296(19)	0.5416(9)	0.75(21)		0.1331(1)	0.6672(5)	0.5411(3)	0.94(4)
O5	16.36	0.0367(5)	0.1967(20)	0.8716(9)	1.12(22)	16.3	0.0370(1)	0.1935(5)	0.8700(3)	1.13(4)
O6		0.2466(5)	–0.2416(19)	0.8582(9)	0.97(23)		0.2471(1)	0.7583(5)	0.8585(3)	0.82(3)
O7		0.1666(4)	0.2332(18)	0.4443(8)	0.59(19)		0.1680(1)	0.2285(5)	0.4464(3)	0.80(3)
O8		0.1324(5)	0.6756(20)	0.3071(9)	1.05(22)		0.1330(1)	0.6707(5)	0.3090(3)	1.02(4)
O9		0.1861(5)	0.3259(20)	0.1584(9)	0.85(22)		0.1864(1)	0.3260(5)	0.1581(3)	0.97(4)
O10		0.0852(5)	0.7237(22)	0.0369(10)	1.55(25)		0.0847(1)	0.7297(6)	0.0395(3)	1.31(4)
O11		0.0506(5)	0.2608(25)	0.1566(10)	1.69(26)		0.0520(1)	0.2556(6)	0.1558(3)	1.30(4)
O12		1/4	0.3369(22)	0	0.59(28)		1/4	0.3353(7)	0	0.91(5)
O13		1/4	0.6495(22)	1/2	0.62(28)		1/4	0.6481(7)	1/2	0.84(5)

TABLE 3. Selected interatomic distances (Å) and geometrical describers for mottanaite-(Ce) and ciprianiite

	mottanaite-(Ce)	ciprianiite		mottanaite-(Ce)	ciprianiite
B1-O4	1.557(14)	1.547(4)	B2-O2	1.557(14)	1.535(4)
B1-O7	1.421(16)	1.414(4)	B2-O6	1.386(16)	1.405(4)
B1-O8	1.560(14)	1.544(5)	B2-O9	1.563(15)	1.525(4)
B1-O13	1.475(13)	1.478(4)	B2-O12	1.473(12)	1.475(4)
<B1-O>	1.503	1.496	<B2-O>	1.495	1.485
TAV	36.9	40.3	TAV	55.3	43.1
TQE	1.0087	1.00092	TQE	1.0129	1.0096
Si1-O1	1.627(9)	1.614(3)	Si2-O8	1.635(10)	1.642(3)
Si1-O2	1.626(9)	1.655(3)	Si2-O9	1.630(9)	1.634(3)
Si1-O3	1.635(10)	1.602(3)	Si2-O10	1.598(11)	1.607(3)
Si1-O4	1.659(9)	1.663(3)	Si2-O11	1.624(11)	1.613(3)
<Si1-O>	1.637	1.633	<Si2-O>	1.622	1.624
TAV	5.7	6.9	TAV	10.9	14.0
TQE	1.0016	1.0017	TQE	1.0027	1.0035
M1-O5	1.937(9)	1.952(3)	M2-O1	2.359(8)	2.380(3)
M1-O10	2.013(11)	1.982(3)	M2-O1	2.366(9)	2.402(3)
M1-O11	1.982(11)	1.964(3)	M2-O3	2.453(10)	2.440(3)
<M1-O>	1.977	1.966	M2-O4	2.596(9)	2.617(3)
OAV	25.0	18.3	M2-O5	2.529(9)	2.508(3)
OQE	1.0075	1.0051	M2-O7	2.437(8)	2.435(3)
			M2-O8	2.552(10)	2.562(3)
M3-O2	2.410(9)	2.434(3)	M2-O11	2.453(9)	2.443(3)
M3-O4	2.622(9)	2.613(3)	<M2-O>	2.468	2.473
M3-O6	2.331(9)	2.338(3)			
M3-O7	2.460(9)	2.428(3)	M4-O2	2.583(9)	2.583(3)
M3-O7	2.516(9)	2.501(3)	M4-O4	2.456(10)	2.429(3)
M3-O8	2.692(10)	2.686(3)	M4-O5	2.399(9)	2.387(3)
M3-O9	2.386(9)	2.386(3)	M4-O6	2.325(9)	2.334(3)
M3-O13	2.371(9)	2.367(3)	M4-O6	2.490(9)	2.476(3)
<M3-O>	2.473	2.469	M4-O9	2.762(9)	2.778(3)
			M4-O10	2.341(10)	2.336(3)
T-O3	1.738(29)	1.884(17)	M4-O12	2.396(9)	2.414(3)
T-O5	1.643(32)	1.615(18)	<M4-O>	2.469	2.467
T-O10	1.858(32)	1.893(18)			
T-O11	1.887(33)	1.916(18)	H-O5		1.11
<T-O>	1.781	1.827			

TABLE 6. Powder diffraction patterns (reflections with I/I_0 > 15, 2θ Cu$K\alpha$ < 60°) calculated for mottanaite-(Ce) and ciprianiite on the basis of the refined structural model

			mottanaite-(Ce)		ciprianiite	
h	*k*	*l*	*d* spacing	I/I_0	*d* spacing	I/I_0
0	0	1	9.569	30	9.586	22
2	0	0	8.886	51	8.877	52
2	0	1	5.590	28	5.580	38
0	1	0	4.746	52	4.729	72
2	1	0	4.186	41	4.174	46
2	1	1	3.618	17	3.608	18
4	0	1	3.571	18	3.564	28
–2	1	2	3.452	67	3.454	79
–2	0	3	3.416	17	3.430	16
4	1	0	3.243	80	3.236	68
–4	0	3	3.187	22	3.204	27
0	0	3	3.190	19	3.195	23
–6	0	1	3.168	16	3.171	23
–4	1	2	3.085	85	3.089	86
2	1	2	2.916	86	2.911	74
4	1	1	2.854	100	2.846	100
–4	1	3	2.646	86	2.653	80
0	1	3	2.647	84	2.648	79
–6	1	1	2.635	84	2.634	84
0	0	4	2.392	21	2.397	21
–8	0	2	2.364	22	2.369	22
0	2	0	2.373	18	2.365	19
–3	1	4	2.252	20		
7	1	0	2.239	21		
6	0	2	2.192	23	2.187	23
3	1	3	2.187	20		
–7	1	3	2.185	18		
6	1	2	1.990	18	1.985	16
4	2	1	1.976	32	1.970	29
–4	2	3	1.903	42	1.903	34
0	2	3	1.904	36	1.901	31
–6	2	1	1.899	39	1.896	35
8	0	2	1.786	16		
4	1	4	1.722	18	1.720	16
–4	0	6	1.708	20	1.715	17
0	2	4	1.685	17		
–6	2	4	1.655	16		
–8	2	2	1.647	21	1.674	16
10	1	0	1.664	23	1.662	21
–10	1	4	1.650	27	1.655	24
–4	1	6	1.607	35	1.612	30
6	2	2	1.610	32	1.606	24

The structures of mottanaite-(Ce) and ciprianiite are very similar to the structure of hellandite-(Ce) described by Oberti et al. (1999). As discussed in detail by Oberti et al. (1999, 2002), REE and actinides have a marked site preference (M2 >> M4 > M3); in particular, actinides and HREE strongly order at the M2 site. The presence of a further tetrahedral site in hellandite (with respect to the structure determined by Mellini and Merlino 1977), which was first reported by Oberti et al. (1999) for hellandite-(Ce), is confirmed also in both crystals studied here. This site is strongly distorted, and is occupied by Be and Li in various proportions. The H atom bonded to the O5 oxygen atom also protrudes into this cavity at ~ 1.0 Å from the O atom. Thus the cavity may host Li and Be at the center, H in an off-centered position, and may also be vacant. The root-name mottanaite defines the hellandite-group samples in which this site is more than half occupied by Li and Be. Accordingly, the sample from Monte Cavalluccio has 1.18 Be + 0.025 Li apfu. Significant amounts of $^{[4]}$(Be,Li) are also present in ciprianiite from Tre Croci, as well as in all the other hellandite occurrences analyzed by Oberti et al. (2002).

Infrared spectra in the OH-stretching region were measured at room temperature with unpolarized light on doubly polished fragments of mottanaite-(Ce). They were acquired (at the University of Roma Tre) with a Nicolet NicPlan microscope equipped with a nitrogen-cooled MCT detector and a KBr beamsplitter. As in the case of hellandite-(Ce) (Oberti et al. 1999), the spectra show a single broad absorption feature centered around 3450 cm^{-1}, thus suggesting a single type of strongly hydrogen-bonded OH in the structure. At closer inspection, the broad absorption band is the sum of several (at least three) overlapping components, as suggested by the presence of defined shoulders at 3490 and 3400 cm^{-1}. This is consistent with a wide variety of OH environments due to local short-range disorder at the next-nearest-neighbor cation sites bonded to O5 (i.e., M1, M2, and M4), and to intra-crystalline chemical variations (see below).

Analogies can be found between the local environment of the OH group in hellandite and that in hydrogarnets, and the O-H vibrational frequency of hellandites is close to that measured (3432 cm^{-1}) for henritermierite, a Mn^{3+}-bearing hydrogarnet. The spectrum of henritermierite, collected at room temperature also shows a very broad band that is resolved into several overlapping components at 80 K; these are assigned to stretching modes of OH groups involved in enhanced hydrogen bonding with the surrounding oxygen atoms (Armbruster et al. 2001).

CHEMICAL COMPOSITION AND RELATIONS TO OTHER HELLANDITE-GROUP MINERALS

The crystals used for the single-crystal X-ray study were mounted in epoxy and then analyzed by electron- and ion-microprobes. WDS-EMP analyses were done with an ARL microprobe. Analytical conditions were 15 kV and 20 nA beam current. Natural minerals were used as standards: fluorite (F*K*α), clinopyroxene KH1 (Si*K*α, Ca*K*α), microcline BH1 (K*K*α), ilmenite BH7 (Fe*K*α, Ti*K*α), and spessartine BH5 (Mn*K*α). The data were processed with the program PROBE 5.2 (Donovan and Rivers 1990), after Phi-Rho-*Z* correction following Armstrong (1988).

SIMS analyses were done with a Cameca IMS 4f ion microprobe. The strong spectral interferences in the REE region were treated as described by Ottolini and Oberti (2000), in which the reader can find the listing of the various standards used and of the procedures followed for elemental quantification from the collected signals. The oxide weight percentages resulting from EMP and SIMS analyses were then used to calculate the unit formulae on the basis of 24 (O + F) atoms (cf. Oberti et al. 1999 for discussion of the stoichiometric constraints in hellandite). Due to the strong intra-crystalline compositional variations, the analyses reported in Table 7 were obtained by averaging a number of analytical points (2 to 4) selected to best fit the average crystal composition obtained by the structure refinements. The excellent agreement between chemical information obtained from the structure refinement (site scattering values in Table 2) and the results of the chemical analyses (calculated group-site scattering in Table 7) testifies to the accuracy of the procedure used to determine the cation site-populations and the OH content. In particular, the SIMS analyses for light elements confirmed the structural constraint OH ≤ (2 – Li – Be – F) (Oberti et al. 1999, 2002).

The ideal structural formula of mottanaite-(Ce) is $^{M3,4}Ca_4\,^{M2}(R^{3+}Ca)^{M1}Al^{T}Be_2Si_4B_4O_{22}{}^{O5}O_2$, where R^{3+} = Y + REE, and Ce dominates over REE. The occupancy of the additional tetrahedral site is balanced by lower contents of trivalent cations at the M2, M3 and M4 sites with respect to hellandite $[^{M3,4}(Ca_3R^{3+})\,^{M2}(R^{3+})_2{}^{M1}Al^{T}\square_2Si_4B_4O_{22}{}^{O5}(OH)_2]$; the low hydrogen contents in mottanaite is correlated with full occupancy of the T site. Because the M2 site is more than half-occupied by REE, a modifier is added to the root-name to specify the dominant REE (Bayliss and Levinson 1988; Oberti et al. 2002).

The ideal structural formula of ciprianiite is: $^{M3,4}Ca_4\,^{M2}[(Th,U)REE]^{M1}Al^{T}{}_2Si_4B_4O_{22}{}^{O5}(OH,F)_2$. In this formula, the tetrahedrally coordinated T site is vacant, and the heterovalent exchange relating ciprianiite to hellandite is $^{M3,4}Ca^{M2}(Th,U)\,^{M3,4}REE_{-1}{}^{M2}REE_{-1}$ (Oberti et al. 2002).

The chondrite-normalized (Cn) patterns for Y, REE, Th, and U of mottanaiite-(Ce) and ciprianiite (normalization-factor C1 of Anders and Ebihara 1982) are broadly similar to the pattern reported by Oberti et al. (1999) for hellandite-(Ce) from the same volcanic region. They decrease linearly from LREE toward HREE with a negative Eu anomaly (Fig. 2). Ciprianiite shows a slightly concave pattern at the LREE-side, with an increase from La to Ce, a flat trend from Ce to Pr, then a linear

TABLE 7. Microchemical analysis and formula unit [on the basis of 24 (OH + F)] for the refined crystals of mottanaiite-(Ce) and ciprianiite

mottanaite-(Ce)				ciprianiite			
Oxides	wt-%	Formula		Oxides	wt-%	Formula	
SiO_2	23.85	Si	3.978	SiO_2	22.94	Si	4.007
B_2O_3	13.85	B	3.987	B_2O_3	13.28	B	4.003
BeO	2.94	Be	1.180	BeO	1.95	Be	0.818
Li_2O	0.037	Li	0.025	Li_2O	0.053	Li	0.037
TiO_2	0.560	Σ [4] sites	9.169	TiO_2	0.730	Σ [4] sites	8.865
Al_2O_3	2.53	Ti	0.070	Al_2O_3	2.33	Ti	0.096
Fe_2O_3	3.06	Al	0.497	Fe_2O_3	2.87	Al	0.479
Cr_2O_3	0.00	Fe^{3+}	0.384	Cr_2O_3	0.015	Fe^{3+}	0.377
Mn_2O_3	0.00	Cr^{3+}	0.000	Mn_2O_3	0.371	Cr^{3+}	0.002
MgO	0.140	Mn^{3+}	0.000	MgO	0.180	Mn^{3+}	0.016
Na_2O	0.00	Mg	0.035	Na_2O	0.00	Mg	0.047
CaO	24.46	Σ M1	0.986	CaO	24.60	Σ M1	1.017
BaO	0.002	Na	0.000	BaO	0.002	Na	0.000
La_2O_3	7.42	Ca	4.371	La_2O_3	1.39	Ca	4.603
Ce_2O_3	12.63	Ba	0.000	Ce_2O_3	5.48	Ba	0.000
Y_2O_3	0.073	La	0.456	Y_2O_3	0.185	La	0.090
Pr_2O_3	1.103	Ce	0.771	Pr_2O_3	0.863	Ce	0.351
Nd_2O_3	2.36	Y	0.006	Nd_2O_3	3.03	Y	0.017
Sm_2O_3	0.137	Pr	0.067	Sm_2O_3	0.332	Pr	0.055
Eu_2O_3	0.020	Nd	0.141	Eu_2O_3	0.051	Nd	0.189
Gd_2O_3	0.094	Sm	0.008	Gd_2O_3	0.139	Sm	0.020
Dy_2O_3	0.024	Eu	0.001	Dy_2O_3	0.049	Eu	0.003
Er_2O_3	0.005	Gd	0.005	Er_2O_3	0.012	Gd	0.008
Yb_2O_3	0.002	Dy	0.001	Yb_2O_3	0.006	Dy	0.003
ThO_2	4.01	Er	0.000	ThO_2	15.80	Er	0.001
UO_2	0.430	Yb	0.000	UO_2	0.872	Yb	0.000
H_2O	0.390	Th	0.152	H_2O	0.465	Th	0.628
F	1.00	U	0.016	F	0.89	U	0.034
O=F	0.421	ΣM2,3,4	5.997	O=F	0.370	ΣM2,3,4	6.000
TOTAL	100.71	F	0.527	TOTAL	98.50	F	0.490
		OH	0.434				
ss at M1 cal	18.4	Σ O5	0.962	ss at M1	19.2	OH	0.543
ss at M2, 3, 4 cal	183.0	Σ (O5, T)	2.166	ss at M2, 3, 4 cal	191.3	Σ O5	1.033
ss at O5 cal	16.5			ss at O5 cal	16.5	Σ (O5, T)	1.888

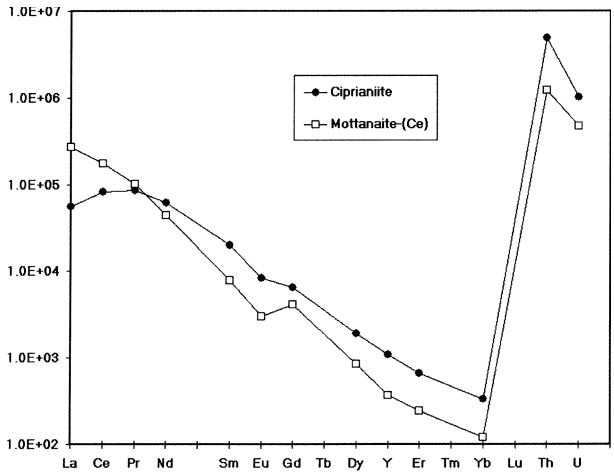

FIGURE 2. Chondrite-normalized patterns of mottanaite-(Ce) and ciprianiite. Experimental data for Th, U, and Y [plotted in the position of Ho (not measured) due to the similarity in their ionic radii] are compared to those of REE.

decrease toward HREE. Comparison of all the available chondritic patterns for samples from different occurrences (Oberti et al. 1999, 2002) shows that hellandite has no selectivity toward incorporation of REE, therefore the composition of the studied samples can be used to monitor the fluid composition during formation of these minerals. We stress that the Cn pattern of ciprianiite is identical in shape to the patterns of titanite (Della Ventura et al. 1999a) and zirconolite (Bellatreccia et al. 2002) from the same locality, which also show concave patterns at the LREE-side. Since both titanite and zirconolite do not show any selectivity toward incorporation of rare-earth elements, the similarity in Cn patterns for different minerals from different host-rocks suggests a constant composition of the hydrothermal/metasomatic fluid (at least with respect to REEs) at the scale of the single volcanic complex.

Textural relationships in the studied ejecta suggest that, as already observed for several other REE- and actinide-bearing minerals in tephra from the Latium volcanic region (Della Ventura et al. 1993, 1996, 1999a, 1999b; Maras et al. 1995; Oberti et al. 2001; Bellatreccia et al. 2002), the genesis is secondary to the formation of the host rock, and can be related to late-stage post-magmatic hydrothermal/metasomatic fluids enriched in these elements. This is also the case for the two hellandite-group minerals described here.

ACKNOWLEDGMENTS

Sincere thanks are due to F. Bellatreccia, E. Bernabè, E. Caprilli, S. Fiori, and F. S. Stoppani, who found and provided samples of the two new hellandite end-members. G.D.V. was supported by the Accademia dei Lincei, Commissione per i Musei Naturalistici e Musei della Scienza, and by MURST 1999 "Cristallochimica delle specie minerali: uso di tecniche avanzate per una moderna sistematica". Financial support by the CNR to the EMP laboratory at the Università di Modena and to the SIMS laboratory at the CSCC is also acknowledged.

REFERENCES CITED

Anders, E. and Ebihara, M. (1982) Solar-system abundances of the elements, Geochimica and Cosmochimica Acta, 46, 2263–2380.

Armbruster, T., Kohler, T., Libowitzky, E., Friederich, A., Miletich, R., Kunz, M., Medenbach, O., and Gutzmer, J. (2001) Structure, compressibility, hydrogen bonding, and dehydration of the tetragonal Mn^{3+} hydrogarnet, henritermierite. American Mineralogist, 86, 147–158.

Armstrong, J.T. (1988) Quantitative analysis of silicate and oxide minerals. Comparison of Monte-Carlo, ZAF and Phi-Rho-Z procedures. Microbeam Analyses, 23, 239–246.

Bayliss, P. and Levinson, A.A. (1988) A system of nomenclature for rare-earth mineral species: revision and extension. American Mineralogist, 73, 422–423.

Bellatreccia, F., Della Ventura, G., Williams, C.T., Lumpkin, G.R., Smith, K.L., and Colella, M. (2002) Non metamict zirconolite polytypoids from the feldspathoid-bearing alkali-syenitic ejecta of the Vico volcanic complex (Latium, Italy). European Journal of Mineralogy, in press.

Bernabè, E. (1987) Probabile tadzhikite sui Monti Cimini. Notiziario di Mineralogia e Paleontologia, 51, 20–22.

Brögger, W.C. (1903) Über der Hellandit, ein neues Mineral. Nyt. Mag. F. Naturv. Kristiania, 41, 213–221 (not seen; extracted from American Mineralogist, 62, 89, 1977).

———(1907) Hellandit von Lindvikskollen bei Kragero, Norwegen. Zeitschrift für Kristallographie, 42, 417–439 (not seen; extracted from American Mineralogist, 62, 89, 1977).

———(1922) Hellandit. Vid. Selsk. Sk. (Oslo). Mat-Nature KI, 6, 1-16 (not seen; extracted from American Mineralogist, 62, 89, 1977).

Della Ventura, G., Di Lisa, A., Marcelli, M., Mottana, A., and Paris, E. (1992) Composition and structural state of alkali feldspars from ejecta in the Roman potassic province, Italy: petrological implications. European Journal of Mineralogy, 4, 411–424.

Della Ventura, G., Parodi, G.C., Mottana, A., and Chaussidon, M. (1993) Peprossiite-(Ce), a new mineral from Campagnano (Italy): the first anhydrous rare-earth-element borate. European Journal of Mineralogy, 5, 53–58.

Della Ventura, G., Mottana, A., Parodi, G.C., Raudsepp, M., Bellatreccia, F., Caprilli, E., Rossi, P., and Fiori, S. (1996) Monazite-huttonite solid-solutions from the Vico Volcanic Complex, Latium, Italy. Mineralogical Magazine, 60, 751–758.

Della Ventura, G., Bellatreccia, F., and Williams, C.T. (1999a) Zr- and REE-rich titanite from Tre Croci, Vico Volcanic complex (Latium, Italy). Mineralogical Magazine, 63, 123–130.

Della Ventura, G., Williams, C.T., Cabella, R., Oberti, R., Caprilli, E., and Bellatreccia, F. (1999b) Britholite-hellandite intergrowths and associated REE-minerals from the alkali-syenitic ejecta of the Vico volcanic complex (Latium, Italy): petrological implications bearing on REE mobility in volcanic systems. European Journal of Mineralogy, 11, 843–854.

De Rita, D., Funiciello, R., Rossi, U., and Sposato, A. (1983) Structure and evolution of the Sacrofano-Baccano caldera, Sabatini volcanic complex, Rome. Journal of Volcanology and Geothermal Research, 17, 219–236.

Donovan, J.J. and Rivers, M.L. (1990) PRSUPR—A PC based automation and analysis software package for wavelength-dispersive electron-beam microanalysis. Microbeam Analysis, 25, 66–68.

Mandarino, J.A. (1981) The Gladstone-Dale relationship: Part IV. The compatibility concept and its application. Canadian Mineralogist, 19, 441–450

Maras, A., Parodi, G.C., Della Ventura, G., and Ohnestetter, D. (1995) Vicanite-(Ce): a new Ca-Th-RE borosilicate from the Vico Volcanic District, Tre Croci, Vetralla (Latium, Italy). European Journal of Mineralogy, 7, 439–446.

Mellini, M. and Merlino, S. (1977) Hellandite: a new type of silicoborate chain. American Mineralogist, 62, 89-99.

Oberti, R., Ottolini, L., Camara, F., and Della Ventura, G. (1999) Crystal structure of non-metamict Th-rich hellandite-(Ce) from Latium (Italy) and crystal chemistry of the hellandite-group minerals. American Mineralogist, 84, 913–921.

Oberti, R., Ottolini, L., Della Ventura, G., and Parodi, G.C. (2001) On the symmetry and crystal chemistry of britholite: new structural and microanalytical data. American Mineralogist, 86, 1066–1075.

Oberti, R., Della Ventura, G., Ottolini, L., Hawthorne, F.C., and Bonazzi, P. (2002) Re-definition, nomenclature and crystal-chemistry of the hellandite-group. American Mineralogist, 87, 745–752.

Oftedal, I. (1964) Contribution to the mineralogy of Norway, no. 24. On the chemical composition of hellandite. Norsk Geologisk Tidsskrift, 44, 35–37 (Not seen; extracted from Canadian Mineralogist, 11, 760.)

———(1965) Über den Hellandit. Tschermaks Mineralogisch-Petrographische. Mitteilungen, 10. 125–129.

Ottolini, L. and Oberti, R. (2000) Accurate quantification of H, Li, Be, B, F, Ba, REE, Y, Th, and U in complex matrixes: a combined approach based on SIMS and single-crystal structure-refinement. Analytical Chemistry, 72, 16, 3731–3738.

Sheldrick, G. M. (1993) SHELX-93. Program for crystal-structure refinement. University of Göttingen, Germany.

Washington, H.S. (1906) The Roman Comagmatic region. Carnegie Institution Washington Publication No. 57, 199 p. Washington, D.C.

MANUSCRIPT RECEIVED JUNE 11, 2001
MANUSCRIPT ACCEPTED JANUARY 7, 2002
MANUSCRIPT HANDLED BY PETER C. BURNS